Enhancing Performance of a Twin-rotor Helicopter Model Using Intelligent Active Force Control

Sherif I. Abdelmaksoud[1]; Musa Mailah[1]; and Ayman M. Abdallah[2]

[1]School of Mechanical Engineering, Faculty of Engineering, Universiti Teknologi Malaysia, 81310 UTM Johor Bahru, Johor, Malaysia
[2]Aerospace Engineering Department, King Fahd University of Petroleum and Minerals, Dhahran 31261, Saudi Arabia

[*]Corresponding email: iasherif@graduate.utm.my

Article history
Received
26th October 2020
Revised
5th April 2021
Accepted
1st June 2021
Published
14th August 2021

ABSTRACT

This paper presents a study on the effectiveness of utilizing an innovative control approach based on an intelligent active force control (IAFC) strategy to stabilize a twin-rotor helicopter model and improve its ability to effectively reject external disturbances via a simulation work. A detailed mathematical model of a two-degrees-of-freedom (DOF) helicopter was derived using the *Euler-Lagrange* method taking into account the effects of coupling and disturbances. In this developed model, a Proportional–Integral–Derivative (PID) controller was designed and combined with the proposed IAFC strategy to yield an intelligent hybrid control architecture known as a PID-IAFC scheme that can improve system performance and reject various types of applied disturbances. The intelligent algorithms used in the schemes were based on iterative learning (IL) and fuzzy logic (FL). In this work, different types of external disturbances in the form of sinusoidal wave, pulsating, and random noise disturbances were applied to the helicopter system to verify the sensitivity and durability of the proposed control schemes and consequently, a comparative study was performed to analyze the system characteristics. Notably, the efficacy of the IAFC based control unit was investigated to improve the body jerk performance in the presence of external disturbances. The acquired results reveal the effectiveness and robustness of the IAFC based controller in stabilizing the dual-rotor helicopter, rejecting the applied disturbances, and improving the body jerk performance by at least 54% for pitching and 19% for yawing motions in the presence of the pulsating disturbance, and 60% and 54%, respectively, for the random noise disturbance.

Keywords: *Twin-rotor system, 2-DOF helicopter, active force control, intelligent systems, self-tuning, iterative learning, fuzzy logic, body jerk performance*

1.0 INTRODUCTION

Unmanned aerial vehicle (UAV) is a widespread topic of interest in recent years. The subject matter receives much attention due to the fact that UAVs have many desirable features including small size and weight, high-mobility, and self-stabilizing allowing them to be used in a wide range of applications such as search and rescue (SAR) mission, remote sensing, real-time monitoring, and meteorological reconnaissance (Abdelmaksoud et al., 2020). Among the different types of UAVs, a twin-rotor helicopter is considered one of the most versatile and vital modes of transportation nowadays. Unlike fixed-wing aircraft, it can take off and land (VTOL) vertically without a runway, hover in one spot, perform quick maneuvering, and fly backward or sideways. Besides, it is also utilized in a wide range of applications in the military and civilian sectors. However, the helicopter is a multi-variable, highly non-linear, and strongly coupled system. It also faces several impediments during tracking certain paths such as instability, moving and fixed obstacles, motors failure,

external disturbances, and model uncertainties. Hence, the existence of a robust and effective control system is deemed necessary. A 2-degrees-of-freedom (DOF) helicopter model is an example of a UAV commonly used as a dual-rotor laboratory experimental rig to practically test the effectiveness of proposed control strategies that may be applied and implemented to a real helicopter system. It consists of two propellers at both ends of an axial beam pivoted on a fixed base which allows it to rotate freely in both the vertical and horizontal planes, as shown in **Figure 1**. The front rotor, which is horizontal to the ground, is the main rotor and causes a pitching moment around the pitch axis, while the back or tail rotor generates a yawing moment around the yaw axis. Both the front and back rotors generate a torque on each other that in turn causes the coupling effect. The beam is driven by two perpendicular propellers actuated by two DC motors. Several research works have been conducted to develop the control techniques for the 2-DOF helicopter over the past decades to provide robust solutions in demanding environments. Among the various impediments encountered by the 2-DOF helicopter system are external disturbances and uncertainties while trajectory tracking. These are considered essential challenges to achieve high performance in different operating and loading conditions.

Figure 1: A 2-DOF helicopter model (Abdelkader and Kais, 2019)

Maiti *et al*. (2018) proposed a particle swarm optimization (PSO) method-based Proportional–Integral–Derivative (PID) controller and utilized a cross-coupling technique. Pandey *et al*. (2018) implemented a PID controller tuned using a bacterial foraging optimization (BFO) technique for solving the stabilizing problem in the presence of actuator nonlinearity, disturbances, and uncertainties, based on *Kharitonov* robust stability criteria. Also, Ijaz *et al*. (2016) designed a fractional order PID (FOPID) controller adjusted using the *Nelder Mead* (NM) optimization method and compared its effectiveness with FOPID tuned using the PSO technique and traditional PID controller. The results showed better effectiveness and less control effort of the NM-based FOPID method compared with other control schemes, in the presence of disturbances. Regarding the linear quadratic regulator (LQR) approach, it has also been proposed to control the attitude and position of a twin-rotor MIMO system (TRMS). Almtireen *et al*. (2018) proposed three linear control designs, full state feedback (FSF), LQR, and PID controller, whereas Choudhary (2016) investigated an optimal control solution by designing a LQR adjusted using a trial-and-error method (TEM). Moreover, the *H-infinity* control scheme has received considerable

attention in controlling the 2-DOF helicopter system because of its effectiveness in rejecting disturbances. A robust fault estimation method has been presented by Witczak *et al*. (2016) using $H\infty$ approach to achieve certain disturbance level attenuation with observer convergence, in the presence of external disturbances and unknown inputs.

For non-linear controllers, many types have been proposed such as the backstepping control (BC) (Rashad *et al*., 2016), sliding mode control (SMC) (Faris *et al*., 2017; Precup *et al*., 2017; Rakhtala and Ahmadi, 2017; Rashad *et al*., 2017; Van, 2016), and feedback linearization (FBL) approach (Lin *et al*., 2018; Chi, 2017). Their results revealed better efficacy and robustness in stabilizing and improving the tracking response in the presence of disturbances, uncertainties, and other impediments. However, they may cause some adverse effects such as chattering leading sometimes to a failure in the entire dynamic system. Ilyas *et al*. (2016) designed first-order SMC and BC schemes for dealing with the oscillations and chattering effects in the pitch and yaw angles in the presence of parametric uncertainties and external disturbances. The results showed better effectiveness of the BC in giving efficient behavior and repelling oscillations and chattering compared to the SMC. Regarding the model predictive control (MPC), Raghavan and Thomas (2017) studied it practically and systematically, for solving the coupling and non-linear consequences to achieve efficient tracking performance. The results presented that the proposed strategy is effective and robust in tracking desired trajectories without violating the control input constraints and rejecting the external disturbances and coupling impacts.

Intelligent controllers attracted many researchers, because of their smart approaches in solving control problems. The application of intelligent control mechanisms to stabilize the rotorcraft UAVs during trajectory tracking has found growing interest. In the work done by Zeghlache and Amardjia (2018), a fuzzy sliding mode control based on the non-linear observer was presented experimentally to control and stabilize a twin-rotor helicopter against coupling, non-linearities, uncertainties, and external disturbances to achieve accurate tracking.

On trajectory tracking in the wake of external disturbances, higher derivatives of motion have been rarely studied. While tracking a path, the twin-rotor helicopter not only experiences the motion due to acceleration but also of higher derivatives like a jerk, jounce (snap), etc. Logically, the acceleration does not begin suddenly, but rather extends from zero datum to a specified state, and therefore there must be some jerks incorporated. In general, designers try to reduce the exposure to an unnecessary or undesirable motion to avoid the negative effects of the vibrational levels and oscillations which may cause a failure in the dynamic systems. Thus, reducing the body jerk is deemed an important concern (Eager *et al*., 2016).

To achieve the desired motions with the ability to fend off disturbances, Yang *et al*. (2016) presented, practically and systematically, a composite control strategy based on an active disturbance rejection control (ADRC) and a feed-forward input shaping technique. Both the analytical and experimental results demonstrated the viability and robustness of the suggested approach compared to the conventional PID controller in rejecting the external disturbances and changes of the parameters. One of the innovative ways related to the control of dynamical systems is the active force control (AFC) technique that was first demonstrated by Hewit and Burdess in the early eighties (Hewit and Burdess, 1981) based on the classical *Newton's* second law of motion. The basic idea of AFC is the appropriate estimation of the inertia/mass parameter of the dynamical system and the accurate measurements of the acceleration and torque/force signals induced by the system (Sabzehmeidani et al., 2021). The AFC technique-based controller can effectively reject any known/unknown, internal/external disturbances, operate in different conditions, and keep the system robust and stable during the system operation (Burdess and Hewit, 1986). It can also be readily combined with classical, modern, or intelligent control systems. Some research works have been reported in (Abdelmaksoud et al., 2020; Omar et al., 2017), which combined analytically the AFC strategy with the PID controller to stabilize the

rotorcraft systems and improve disturbance rejection capability whereas, in the work done by (Abdelmaksoud et al., 2021; Ramli et al., 2013; Meon et al., 2012), the AFC-based control strategy was proposed for a 2-DOF helicopter model to compensate for the disturbances where the simulated results showed the effectiveness and robustness of the AFC-based technique.

The main contribution of this paper is to analytically propose an innovative hybrid control structure based on an intelligent active force control (IAFC) strategy to stabilize a twin-rotor helicopter system, fend off undesired disturbances, and effectively improve the body jerk performance while performing a trajectory tracking task in demanding environments.

The remainder of this paper is organized as follows: Section 2 describes the mathematical model of a 2-DOF helicopter system under specific assumptions. Then, the designed PID controller and proposed IAFC technique with iterative learning and fuzzy logic are presented in Section 3. Section 4 presents the simulation results and performance analysis for the trajectory tracking tests based on the prescribed operating and loading conditions. Finally, the paper's conclusion is given in Section 5.

2.0 MODELING THE SYSTEM DYNAMICS

In the following sections, the mathematical model of a 2-DOF helicopter system was derived based on the *Euler-Lagrange* approach considering the coupling effects and various types of disturbances.

2.1. 2-DOF Helicopter System Modeling

The mathematical model of the 2-DOF helicopter model was derived according to works done by (Harshath *et al*. 2016). The 2-DOF helicopter platform is shown in **Figure 2** where it was derived based on the following assumptions (Xin *et al*., 2019):

1. The main and back rotors are of the same size and equidistant from each other.
2. The model is horizontal and parallel with the ground when the pitch angle is zero.
3. The pitch angle increases positively when the front rotor is moved upwards, the body rotates CCW about the *y*-axis, and the front rotor voltage is positive.
4. The yaw angle increases positively when the body rotates CCW about the *z*-axis and the back-rotor voltage is positive.
5. As the system is fixed, it cannot rotate around the roll axis or move along the axis.

To derive the model of the 2-DOF helicopter, it is necessary to study the behavior of the center of mass where it displaces a distance, $l$cm on the *x*-axis as shown in **Figure 2**. Thus, the center of mass after the transformation of the coordinates, utilizing the pitch and yaw rotation matrices is as follows:

$$\begin{aligned} X\text{cm} &= l\text{cm}\cos\psi\cos\theta \\ Y\text{cm} &= l\text{cm}\sin\psi\cos\theta \\ Z\text{cm} &= l\text{cm}\sin\theta \end{aligned} \qquad (1)$$

Where θ and ψ are the pitch and yaw angles, respectively while $l$cm is the distance of the center of mass and intersection of the pitch and yaw axes.

The center of mass is represented by the *Cartesian* coordinates with respect to

the pitch and yaw angles. Based on the *Euler-Lagrange* formulation and the free body diagram of the 2-DOF helicopter in **Figure 2**, the total potential energy (*PE*) of the system due to gravity is:

$$PE = m_{\mathrm{h}} g l_{\mathrm{cm}} \sin\theta \tag{2}$$

The total kinetic energy (*KE*) with reference to **Figure 2**, is the combination of the rotational kinetic energies acting on the pitch and yaw axes, respectively along with the translational kinetic energy generated by the movement of the center of mass is given by:

$$\begin{aligned} KE = {} & \frac{1}{2} J_{\theta} \dot{\theta}^2 + \frac{1}{2} J_{\psi} \dot{\psi}^2 \\ & + \frac{1}{2} m_{\mathrm{h}} \Big[\left(-\sin(\psi)\dot{\psi}\cos(\theta) l_{\mathrm{cm}} - \cos(\psi)\sin(\theta)\dot{\theta} l_{\mathrm{cm}} \right)^2 \\ & + \left(-\cos(\psi)\dot{\psi}\cos(\theta) l_{\mathrm{cm}} + \sin(\psi)\sin(\theta)\dot{\theta} l_{\mathrm{cm}} \right)^2 \\ & + \cos(\theta)^2 \dot{\theta}^2 l_{\mathrm{cm}}^2 \Big] \end{aligned} \tag{3}$$

Where,

J_{θ}, J_{ψ}	:	total moment of inertia about the pitch and yaw axes, respectively
m_{h}	:	total moving mass
g	:	acceleration due to gravity

The torques generated at the pitch and yaw axes are a function of the voltages applied to the motors, such that:

$$\begin{aligned} \tau_{\theta}(t) &= K_{\theta\theta} u_{\theta}(t) + K_{\theta\psi} u_{\psi}(t) \\ \tau_{\psi}(t) &= K_{\psi\theta} u_{\theta}(t) + K_{\psi\psi} u_{\psi}(t) \end{aligned} \tag{4}$$

Where,

$\tau_{\theta}(t), \tau_{\psi}(t)$	:	control torques act on the pitch axis and yaw axis, respectively
$u_{\theta}(t), u_{\psi}(t)$	:	control actions applied as motor voltages to the pitch and yaw rotors, respectively
$K_{\theta\theta}$	:	torque thrust gain from the pitch rotor
$K_{\theta\psi}$	:	cross-torque thrust gain acting on the pitch from the yaw rotor
$K_{\psi\theta}$	:	cross-torque thrust gain acting on the yaw from the pitch rotor
$K_{\psi\psi}$	:	torque thrust gain from the yaw rotor

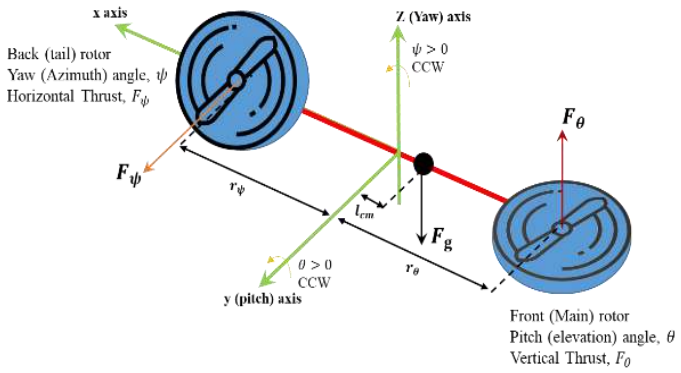

Figure 2: Free-body diagram of the 2-DOF helicopter model.

The generalized forces vector is given by:

$$\begin{aligned} Q = [Q_1, Q_2] = \big[& K_{\theta\theta} u_{\theta}(t) + K_{\theta\psi} u_{\psi}(t) - D_{\theta}\dot{\theta}(t), K_{\psi\theta} u_{\theta}(t) + K_{\psi\psi} u_{\psi}(t) \\ & - D_{\psi}\dot{\psi}(t) \big] \end{aligned} \tag{5}$$

Where D_{θ} and D_{ψ} are the damping about the pitch and yaw axes, respectively. From the *Lagrangian* of the system, the non-conservative forces of the system are written as:

$$\begin{aligned} L &= KE - PE \\ \frac{\partial}{\partial t}\frac{\partial L}{\partial \dot{q}_1} - \frac{\partial}{\partial q_1}L &= Q_1 \\ \frac{\partial}{\partial t}\frac{\partial L}{\partial \dot{q}_2} - \frac{\partial}{\partial q_2}L &= Q_2 \end{aligned} \quad (6)$$

Where,

q_1 and q_2 : generalized coordinates related to θ and ψ, respectively

L : *Lagrange* equation which is the difference between the total kinetic and total potential energies of the system

Based on the *Euler-Lagrange* formulation, the non-linear dynamic equation that describes the motions of the pitch and yaw attitude relative to the motor are given as (Xin *et al*., 2019):

$$(J_\theta + m_h l_{cm}^2)\ddot{\theta} + D_\theta\dot{\theta} + \delta + \beta = K_{\theta\theta}u_\theta + K_{\theta\psi}u_\psi \quad (7)$$

Where,

$\delta = m_h l_{cm}^2 \dot{\psi}^2 \sin(\theta)\cos(\theta)$

$\beta = m_h g l_{cm}\cos(\theta)$

$$\left(J_\psi + m_h l_{cm}^2 \cos(\theta)^2\right)\ddot{\psi} + D_\psi\dot{\psi} - \gamma = K_{\psi\theta}u_\theta + K_{\psi\psi}u_\psi \quad (8)$$

Where,

$\gamma = 2m_h l_{cm}^2 \sin(\theta)\cos(\theta)\dot{\theta}\dot{\psi}$

Defining the state vector of the 2-DOF helicopter model as follows:

$$X = [x_1\ x_2\ x_3\ x_4] \quad (9)$$

Where it represents the DOF as follows:

$$X = [\theta\ \psi\ \dot{\theta}\ \dot{\psi}] \quad (10)$$

The state-space representation is expressed as:

$$[\dot{X}] = \begin{bmatrix} x_3 \\ x_4 \\ \dfrac{K_{\theta\theta}u_\theta + K_{\theta\psi}u_\psi - D_\theta x_3 - m_h l_{cm}^2 {x_4}^2 \sin(x_1)\cos(x_1) - m_h g l_{cm}\cos(x_1)}{(J_\theta + m_h l_{cm}^2)} \\ \dfrac{K_{\psi\theta}u_\theta + K_{\psi\psi}u_\psi - D_\psi x_4 + 2m_h l_{cm}^2 \sin(x_1)\cos(x_1)x_3 x_4}{\left(J_\psi + m_h l_{cm}^2\cos(x_1)^2\right)} \end{bmatrix} \quad (11)$$

The schematic block diagram of a 2-DOF helicopter model is shown in **Figure 3**.

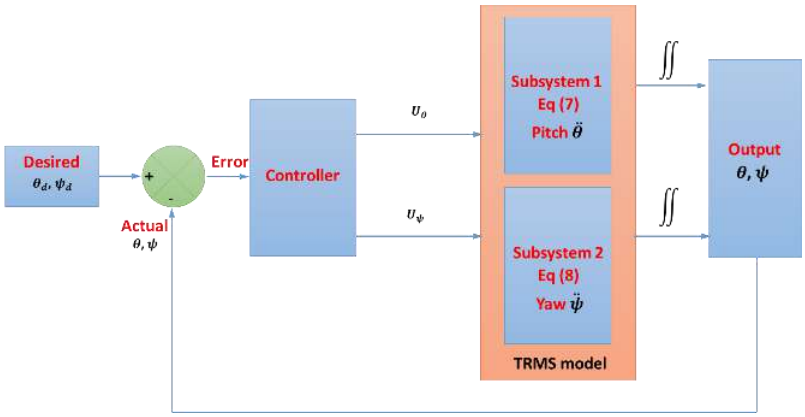

Figure 3: The schematic block diagram of a 2-DOF helicopter model.

2.2. Body Jerk

Jerk is the rate of change in acceleration because of a change in the force. From a mathematical point of view, it is the time derivative of the acceleration (a third derivative of the position). The body jerk (J) can be expressed as:

$$J = \frac{da}{dt} = \frac{d}{dt}(\ddot{\vartheta}) = \frac{1}{I}\frac{d}{dt}(\tau) \tag{12}$$

Where

ϑ : rotational angle
I : moment of inertia
τ : summation of torques

III. CONTROL SYSTEM DESIGN

In this section, after deriving the mathematical model of the 2-DOF helicopter system, the proposed IAFC based control schemes, namely, the AFC with iterative learning (IL) (PID-AFC-IL), fuzzy logic (FL) (PID-AFC-FL), and self-tuning (ST) (ST-PID-AFC) were designed, developed and compared with the PID and PID-AFC control systems to analyze their effectiveness during trajectory tracking as demonstrated in the ensuing sections.

3.1. Proportional–Integral–Derivative (PID)

A PID controller is a relatively robust linear controller that is very popular in the industry and can be employed in a wide range of linear and nonlinear applications due to its simplicity and reliability. The PID principally consists of three gains (controller parameters); the proportional term (K_P) that describes the current error, the integral term (K_I) which expresses the accumulated past error and the derivative term (K_D) that predicts the future error for providing the best control signal. The schematic diagram of the PID control system is shown in **Figure 4**.

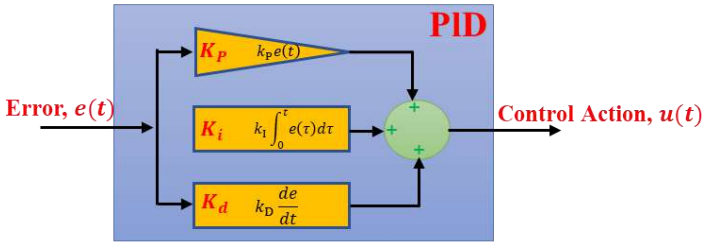

Figure 4. Schematic diagram of a PID controller

To design a PID controller, generally, the following equation is utilized:

$$G(s) = K_P + \frac{K_I}{s} + K_D s \tag{13}$$

Therefore, the output signal of the PID controller can be expressed as:

$$m(s) = G(s)e(s) = K_{\mathrm{P}}e(s) + \frac{K_{\mathrm{I}}e(s)}{s} + K_{\mathrm{D}}se(s) \tag{14}$$

Where $e(s)$ is the error and defined as:

$$e(s) = \text{Reference} - \text{Output} \tag{15}$$

Based on the mathematical model of the 2-DOF helicopter, a PID controller was designed for the yaw angle whereas a PID control system with a feed-forward term was considered to regulate the pitch angle. The non-linear feed-forward term for the pitch angle compensates for the gravitational torque $\beta = m_{\mathrm{h}}gl_{\mathrm{cm}}\cos(\theta)$ in equation (7) and plays a major role in hovering the helicopter at the desired position. It can be expressed as:

$$u_{ff} = k_{\mathrm{ff}}\frac{m_{\mathrm{h}}gl_{\mathrm{cm}}\cos(\theta)}{K_{\mathrm{PP}}} \tag{16}$$

Where k_{ff} is the feed-forward control gain and is equal to 1.0 if it is to be considered; otherwise, it assumes a zero value.

3.2. Intelligent Active Force Control (IAFC)

The AFC strategy is an effective method that basically depends on the appropriate estimation of the estimated inertia (or mass) of the system dynamics and the accurate measurements of the torque (or force) and acceleration signals of the physical system (plant) as shown in **Figure 5**. Therefore, the value of the estimated inertia plays a dominant role in improving the performance of the AFC strategy. It can be found using a crude approximation or intelligent methods (Mailah, 1998). In this work, the AFC parameter was obtained using artificial intelligence (AI) methods incorporating IL and FL and thus, it is defined as IAFC. The open-loop transfer function (TF) of the plant can be obtained by considering the following expression:

$$TF = \frac{\text{output}}{\text{input}} = \frac{\alpha}{T} \tag{17}$$

Where

T : torque applied to the system
α : angular acceleration

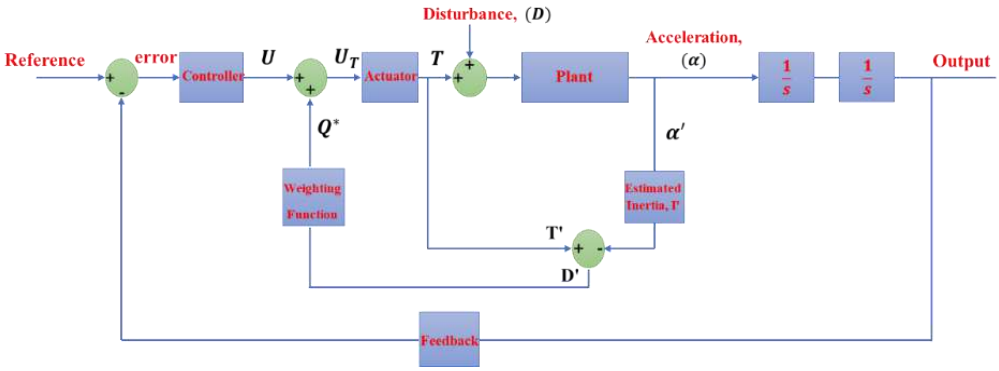

Figure 5. Schematic diagram of the AFC technique.

If the external disturbances are applied to the dynamic system:

$$TF = \frac{\alpha}{T + D} \tag{18}$$

Implementing the AFC strategy:

$$TF = \frac{\alpha}{U_{\mathrm{T}} + D} = \frac{\alpha}{U + Q^{*} + D} \tag{19}$$

Where

U_{T} : total control output signal
U : controller output signal
D : disturbance applied to the system
Q^* : AFC output signal such that $Q^* = WF * D'$
D' : estimated disturbance torque,
WF : weighting function

$$D' = T' - I'\alpha' \tag{20}$$

Where
T' : measured torque
I' : estimated mass moment of inertia
α' : measured angular acceleration

The superscript ($'$) means the measured, estimated, or computed parameters. T' and α' are measurable quantities that can be measured using a torque sensor and an accelerometer, respectively. As a DC motor was assumed as the actuator, equation (20) can be expressed as:

$$D' = I_{\mathrm{t}}K_{\mathrm{t}} - I'\alpha' \tag{21}$$

Where I_{t} is the motor current and K_{t} is the motor torque constant. In this study, two intelligent methods were employed for tuning the AFC strategy, namely, iterative learning (IL) and fuzzy logic (FL), which are basically demonstrated in the following sections.

3.3. Iterative Learning Control (ILC)

ILC is a type of adaptive intelligent control that acts smartly by emulating the function of human brain learning to enhance the automatic control system and achieve better performance. It relies on improving the transient response of the dynamic systems that operate repeatedly over a fixed period (Arimoto *et al*., 1986). It also enhances the system performance using the prior information of the previous iterations (Xu and Tan, 2003). It is important to implement an algorithm to generate the next control input in such a way that the error is gradually reduced or converged on successive trails. Due to the similarity of the mathematical expression associated with the classical PID controller, the IL algorithm could be duly described as P, PI, PD, or PID-type IL algorithm (Arimoto *et al*., 1986), as shown in **Figure 6**. In the work done by (Mascaró Palliser *et al*., 2017), the IL algorithm was applied to a TRMS model to achieve a high execution within a trajectory tracking and the results revealed the capability of the ILC to improve the system performance, efficiently.

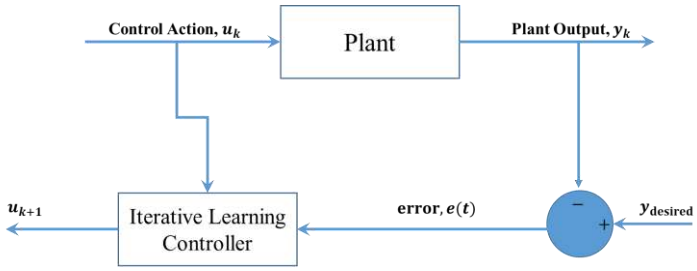

Figure 6. Schematic diagram of the ILC technique.

The learning control rule for a PID-type IL algorithm can be expressed mathematically as (Arimoto *et al*., 1986):

$$u_{\mathrm{k+1}}(t) = u_{\mathrm{k}}(t) + Ke_{\mathrm{k}}(t) \tag{22}$$

Where
$u_{\mathrm{k+1}}(t)$: next step value of the output
$u_{\mathrm{k}}(t)$: current value of the output
$e_{\mathrm{k}}(t)$: current value of the error
K : designed parameter (constant) containing the PID term,

$$K = \phi + \Gamma \int dt + \psi \frac{d}{dt} \tag{23}$$

ϕ, Γ, and ψ: learning parameters associated with the P, I, and D terms, respectively.

In this study, a PD-type IL algorithm was utilized and embedded into the AFC loop to compute the appropriate value of the estimated inertia matrix (*IN*) automatically, according to:

$$IN_{k+1} = IN_k + Ke_k(t) \quad (24)$$

Where
IN_{k+1} : next step value of the estimated inertia
IN_k : current value of the estimated inertia
$K = \phi + \psi \frac{d}{dt}$ (PD-type IL algorithm)

The schematic block diagram of the PID-AFC-IL is shown in **Figure 7**.

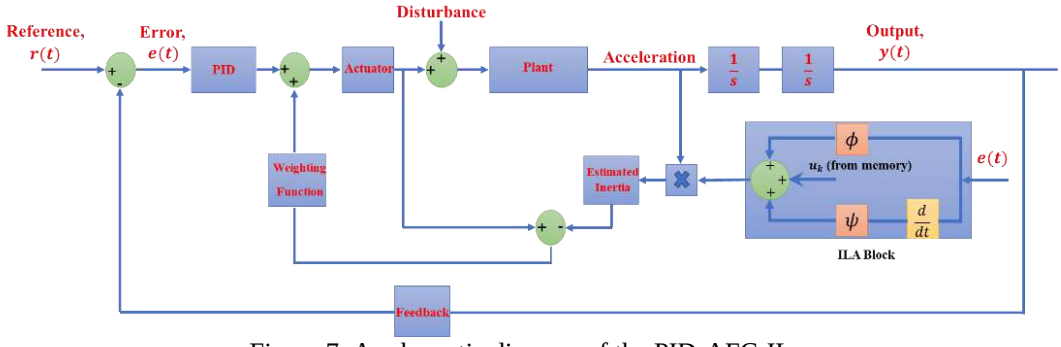

Figure 7. A schematic diagram of the PID-AFC-IL.

3.4. Fuzzy Logic Control (FLC)

FLC is a type of intelligent control method that was first introduced by Lotfi Zadeh in 1965. Its principle is based on the fuzziness in the real-world and simulation of human experience by incorporating the linguistic variables and IF-THEN rules. It is distinguished among other intelligent methods by using human self-thinking during controller design to solve problems, which makes it very suitable for complex dynamic systems, highly non-linear, or incomplete information systems without the need for deep theoretical knowledge. To implement it, there are two main fuzzy implications – the *Mamdani* type and *Takagi-Sugeno* rules. In this study, the *Mamdani* type rule was used for designing the FLC as a tuning tool. There are four basic steps to implement the FLC; 1. ***Fuzzification*** which converts the crisp value into fuzzy value; 2. ***Ruled Evaluation*** which produces the output based on certain rules; 3. ***Aggregation*** which combines the consequences of each rule into a single fuzzy set output, and eventually, 4. ***Defuzzification*** which converts the fuzzy output into a crisp output. The FLC has been proposed to control the 2-DOF helicopter similar to what has been done by Hashim and Abido (2015) and Zeghlache *et al*. (2014). The results revealed the effectiveness of the proposed strategy with particular reference to the convergence speed and solution quality. In this study, FL was employed for the AFC strategy to compute the estimated inertia automatically, and for self-tuning the PID parameters based on the prescribed conditions.

3.4.1. Self-tuning AFC (PID-AFC-FL)

In this section, the FL was combined with the proposed AFC strategy to obtain the estimated inertia automatically. Here, the FL system has two inputs - the error $e(t)$ and actual response $y(t)$ while it has only one output, the estimated inertia value IN). The rule-based inferences applied in the AFC-FL system were also suggested based on the user expert experience as shown in **Table 1**. The linguistic variables used for the error, actual response, and estimated inertia were defined as [Small (S), Medium (M), Large (L)]. The triangular membership function was applied for all variables while the centroidal technique was utilized for the defuzzification using the *Mamdani* engine. The schematic block diagram of PID-AFC-FL is shown in **Figure 8**.

Table 1. IN rule-based inferences applied to the AFC-FL scheme

	IN		
	$y(t)$		
	S	M	L

	S	L	L	M
$e(t)$	M	L	M	M
	L	M	M	S

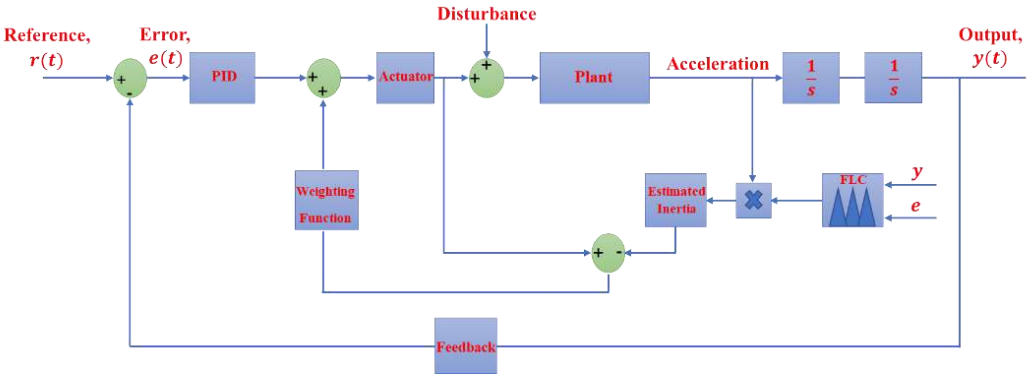

Figure 8. A schematic diagram of the PID-AFC-FL.

3.4.2. Self-tuning PID controller (ST-PID-AFC)

In this work, The PID controller as the main control system was tuned using the FL for providing the automatic adjustment of its control parameters based on the given loading and operating conditions. The self-tuning fuzzy PID controller was proposed based on works by Zhao (1993). Here, the FL system has two inputs - the error and derivative of the error whereas it has three outputs namely, K_P, K_D, and ρ. The error $e(t)$ is the difference between the setpoint and actual responses while the derivative of the error $\dot{e}(t)$ is the rate of the error. Based on equation (13), another equivalent form of the PID control algorithm can be expressed as (Zhen-Yu Zhao *et al*., 1993):

$$G(s) = K_P(1 + \frac{1}{T_i s} + T_d s) \tag{25}$$

Where

T_i : integral time constant $= \frac{K_P}{K_I}$

T_d : derivative time constant $= \frac{K_D}{K_P}$

The relationship between the derivative and integral time constants can be expressed as follows:

$$T_i = \rho T_d \tag{26}$$

By substituting and rearranging the previous equation:

$$K_I = {K_P}^2/\rho K_D \tag{27}$$

The rule-based inferences applied in the ST-PID-AFC scheme were proposed based on the user expert knowledge and experience where the rule-based inferences of K_D can be seen in **Table 2**. Both the linguistic variables used for the error, derivative of error, and ρ were defined as [Very Small (VS), Small (S), Medium (M), Large (L), Very Large (VL)] whereas K_P and K_D were defined as [Big (B) and Small (S)]. Meanwhile, the triangular membership function was applied for all variables while the center of gravity technique was employed for defuzzification in the *Mamdani* engine. The schematic block diagram of the ST-PID-AFC scheme is shown in **Figure 9**.

Table 2. K_D rule-based inferences applied into the ST-FPID scheme

		K_D				
		$\dot{e}(t)$				
		VS	S	M	L	VL
$e(t)$	VS	B	B	B	B	B
	S	S	B	B	B	S

	M	S	S	B	S	S
	L	S	B	B	B	S
	VL	B	B	B	B	B

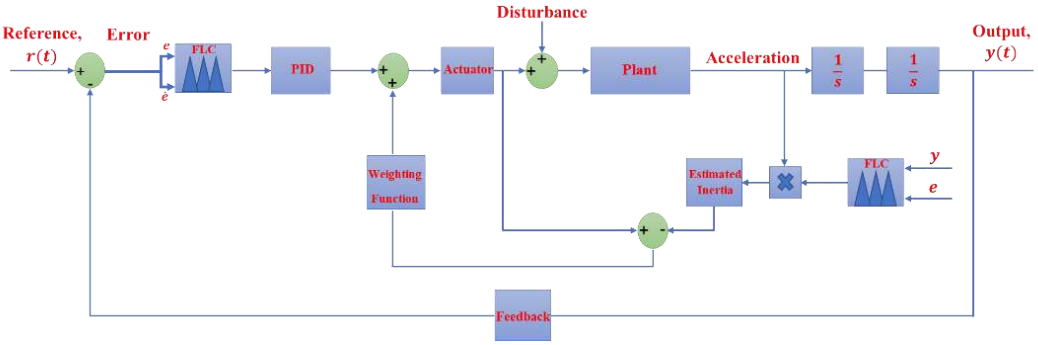

Figure 9. A schematic diagram of the ST-PID-AFC.

Moreover, with regard to the stability analysis of the PID-AFC scheme, it was proven that the stability of the control system is independent of the 2-DOF helicopter model; however, it just depends on the actuator dynamics, PID parameters, and estimated inertia of the AFC strategy. Thus, the stability condition of the 2-DOF helicopter model will not affect the stability of the whole system. Also, this is a guarantee that the system displays responses that are limited when excited with proper inputs to the system (Tahmasebi *et al*., 2017).

IV. SIMULATION, RESULTS, AND DISCUSSION

4.1. Simulation

In this section, the derived dynamic system and proposed control strategies were implemented and simulated using the MATLAB/Simulink software while the Fuzzy Logic Toolbox was used to apply the FLC and self-tuning fuzzy aspects. A number of IAFC-based control schemes, namely, PID-AFC-IL, PID-AFC-FL, and ST-PID-AFC were first developed and later simulated and compared with the PID and PID-AFC systems for benchmarking to analyze the system performance based on their effectiveness and also robustness with the dynamical system tested under various operating conditions. External disturbances were deliberately introduced into the 2-DOF helicopter system in the form of forces and moments to give the effect of a stormy environment. The helicopter model was subjected to three different types of disturbances, namely, sinusoidal wave, repeated disturbance of equal magnitudes and intervals (pulsating), and random noise disturbances, as shown in **Figure 10**.

The amplitude and frequency of the sinusoidal wave were set to 5 rad and 0.08 Hz, respectively whereas the amplitude, period, pulse width, and delay for the pulsating disturbance were assigned as 10 rad, 2 s, 30 % of the period, and 1 s, respectively. The minimum and maximum of the random noise disturbances were fixed to -10 and 10 rad, respectively. The numerical values of the 2-DOF helicopter parameters are listed in **Table 3**, while the PID controller gains tuned heuristically are shown in **Table 4**. The expected results were analyzed in the time domain, noting that the objective of the control system parameters tuning is to minimize the peak time (TP), settling time (TS), overshoot (O), and steady-state error (SSE) for a step input (setpoint) of 20°.

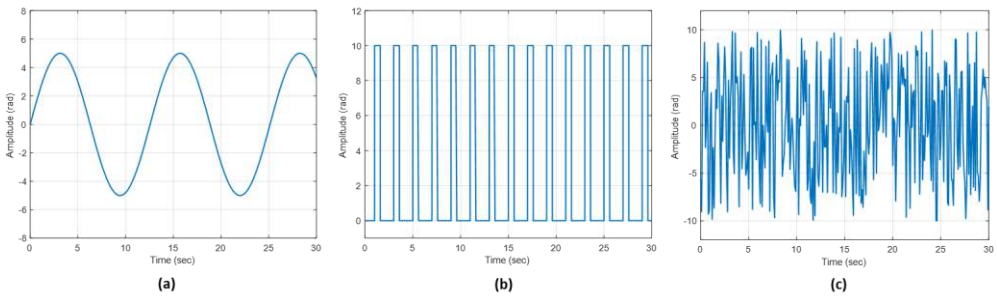

Figure 10. (a) sinusoidal wave, (b) pulsating, and (c) random noise disturbances

Table 3. Twin-rotor helicopter parameters (Xin *et al*., 2019)

Twin-rotor helicopter parameters	**Value**
Gravitational acceleration (m/s^2)	9.81
Thrust torque constant of pitch axis from pitch propeller (Nm/V), K_{pp}	0.2040
Thrust torque constant of yaw axis from yaw propeller (Nm/V), K_{yy}	0.0720
Cross-torque thrust constant of yaw axis from pitch propeller, (Nm/V), K_{yp}	0.0219
Cross-torque thrust constant of pitch axis from yaw propeller, (Nm/V), K_{py}	0.0068
Pitch viscous damping constant (Nms/rad), D_{p}	0.8
Yaw viscous damping constant (Nms/rad),D_{y}	0.318
Total moving mass of the helicopter (kg), m_{h}	1.3872
Center of mass length of the helicopter body from the pitch axis (m), L_{cm}	0.186
Equivalent moment of inertia about pitch axis (kgm^2), J_{p}	0.0384
Equivalent moment of inertia about yaw axis (kgm^2), J_y	0.0432

Table 4. PID controller parameters for various types of motion

PID gains	K_{P}	K_{I}	K_{D}
Pitch	55	30	15
Yaw	65	35	25

4.2. Results and Discussion

In this section, a comparative study of all proposed control systems in the time domain was conducted where simulation works were solved using *ode45* with a variable-step solver, and relative tolerance of 0.001. To evaluate the ability of the proposed controllers, three types of external disturbances were introduced into the 2-DOF helicopter system, namely, the sinusoidal wave, pulsating, and random noise disturbances. All proposed control schemes were also simulated under the same initial conditions. The pitch control voltage was bounded by a saturation block of $u_{\theta\ \max} = 24$ V and $u_{\theta\ \min} = -24$ V whereas the yaw control voltage was limited by a saturation block of $u_{\psi\ \max} = 15$ V and $u_{\psi\ \min} = -15$ V (Xin *et al*., 2019). As mentioned earlier, the rotation of the pitching angle is limited to 40.5° up and -40.5° down while the yaw angle rotation is full, i.e. 360°. The summary of system performances for all control strategies is shown in **Figures 11 to 13** whereas the system characteristics for all cases are demonstrated in **Tables 5 and 6**.

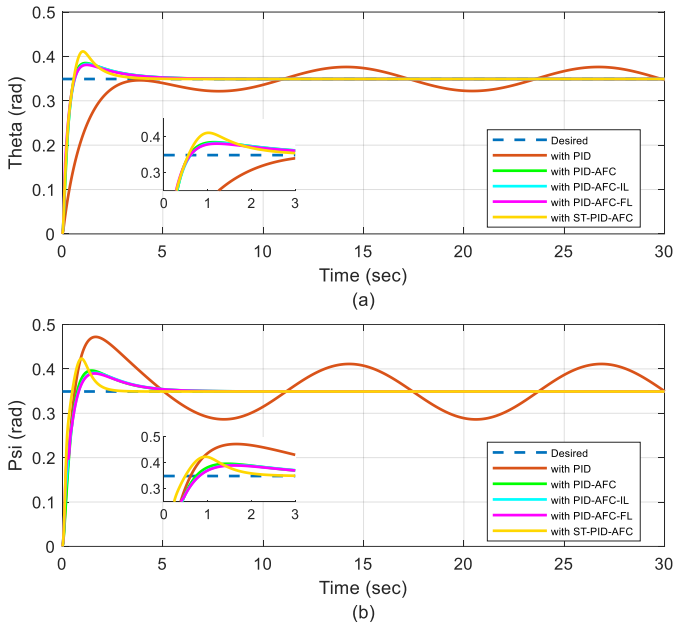

Figure 11. Time responses of all the control schemes in the presence of sinusoidal wave disturbance for the motions related to (a) pitch and (b) yaw of the UAV

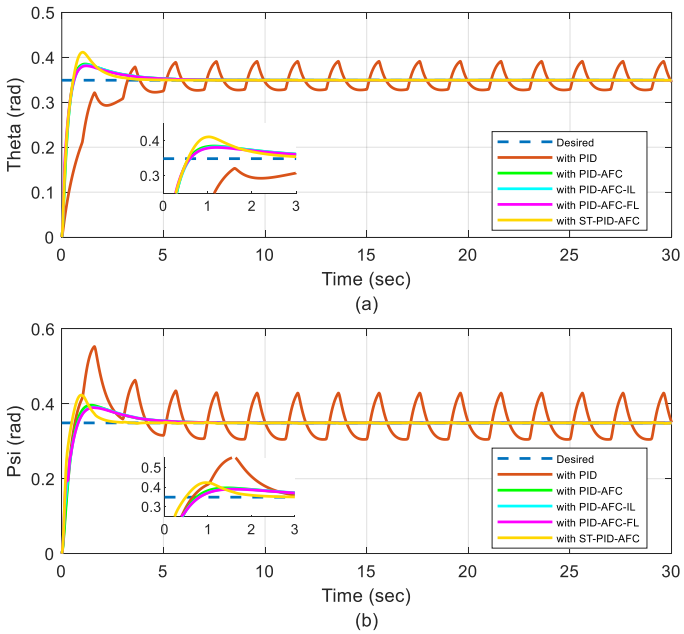

Figure 12. Time response of all the control schemes in the presence of pulsating disturbance for the motions related to (a) pitch and (b) yaw of the UAV

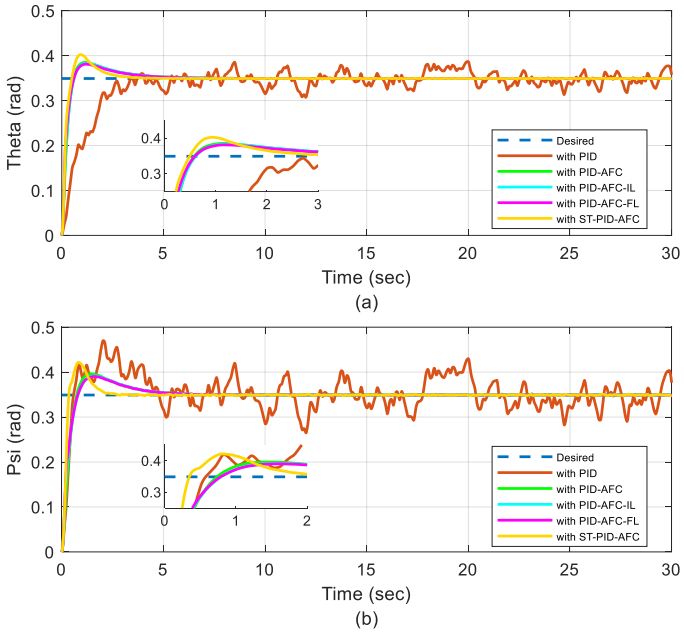

Figure 13. Time response of all the control schemes in the presence of random noise disturbance for the motions related to (a) pitch and (b) yaw of the UAV

From **Figures 11** to **13**, it is clear that despite the popularity of the PID controller in the industry due to its simplicity, it cannot repel the applied disturbances effectively because of its well-known limited capability. On the other hand, AFC-based control schemes show to be more effective and robust in the presence of various types of disturbances and uncertainties in comparison to the traditional PID controller where they seamlessly converge to the desired referenced trajectories in a finite time. The PID response shows a significant degree of oscillations, considerable overshooting, and instability. Starting with the PID-AFC strategy, the system response shows efficacy in rejecting the applied disturbances despite using the crude approximation method when adjusting the estimated inertia value, thereby affirming the strength of the AFC-based strategy. Considering integration with the AI components, all the proposed PID-AFC-IL, PID-AFC-FL, and ST-PID-AFC structures appear much more responsive in stabilizing the 2-DOF helicopter and efficiently rejecting external disturbances with slight changes in their behavior among them. The PID-AFC-IL unit shows the ease of design, efficiency, and automatic setting of its control parameters while applying the stopping criterion for optimizing the estimated inertia value. It is worth noting that, for real-time implementation, the AFC-IL-based controller is considered an efficient control system due to its algorithm simplicity (light numerical computation) and its ability to set its control parameters automatically and online, unlike some other algorithms whose control parameters need to be set off-line.

Table 5. Characteristics of the proposed control schemes for pitching motion

	Sinusoidal wave Disturbance				Pulsating Disturbance				Random Noise Disturbance			
	Settling Time	Overshoot	Peak Time	Steady state Error	Settling Time	Overshoot	Peak Time	Steady state Error	Settling Time	Overshoot	Peak Time	Steady state Error
PID	29.4	8.4	26.7	0.0022	29.9	13.3	29.6	0.0039	29.9	8.2	19.9	0.0085
PID-AFC	3.9	10.3	1.1	2.2 E-05	3.9	10.3	1.1	7.1 E-05	3.9	10.4	1.1	2.6 E-04
PID-AFC-IL	3.9	9.7	1.2	1.7 E-05	3.9	9.8	1.2	6.3 E-05	4	9.8	1.2	2.5 E-04
PID-AFC-FL	3.8	9.1	1.2	1.8 E-05	3.8	9.1	1.2	6.4 E-05	3.8	9.2	1.1	2.6 E-04
ST-PID-AFC	2.8	17.8	1.02	1.2 E-05	2.8	17.8	1.03	3.2 E-05	2.6	15.3	0.9	4.6 E-04

Table 6. Characteristics of the proposed control schemes for yawing motion

	Sinusoidal wave Disturbance				Pulsating Disturbance				Random Noise Disturbance			
	Settling Time	Overshoot	Peak Time	Steady state Error	Settling Time	Overshoot	Peak Time	Steady state Error	Settling Time	Overshoot	Peak Time	Steady state Error
PID	29.7	35.01	1.6	6.4 E-04	29.9	57.8	1.6	0.0014	29.9	24.9	2.04	0.0274
PID-AFC	4.5	13.5	1.4	5.4 E-05	4.5	13.6	1.4	1.9 E-04	4.6	13.5	1.4	3.9 E-04

PID-AFC-IL	4.6	12.1	1.6	3.4 E-05	4.6	12.1	1.6	1.4 E-04	4.6	12.3	1.6	4.1 E-04
PID-AFC-FL	4.5	11.6	1.6	3.7 E-05	4.5	11.7	1.5	1.4 E-04	4.6	11.9	1.6	4.3 E-04
ST-PID-AFC	2.1	21.2	0.9	2.5 E-05	2.1	21.2	0.9	1.05 E-04	2.1	21.4	0.8	0.0016

Regarding the PID-AFC-FL approach, one of the exceptional benefits of using the FL is that it does not require any precise mathematical formulation or model; the user experience is the only typical pre-requisite to implement it. It also smoothly converges to the desired setpoint without any overshooting on the response. For the ST-PID-AFC scheme, the results exhibit the proposed strategy's ability to stabilize the helicopter model and impressively reject the outside unsettling influences. Referring to **Tables 5 and 6**, compared to the proposed control schemes, the ST-PID-AFC system shows better performance in terms of the settling time, peak time, and steady-state error with tolerable overshoot with respect to the control saturation from others. It is considered one of the best options among other proposed control methods in cases that do not include prior knowledge of the control or dynamic system parameters, different loading and operating conditions, and unspecified disturbances in unknown environments. Further, in all previous cases, the PID controller parameters were tuned using the heuristic method that requires many trials and longer time to reach 'optimized' values of the gains but in this case, the ST-PID controller can adjust its parameters automatically depending on the prescribed environment and surrounding conditions.

In this work, the efficacy of utilizing the IAFC-based controller on the body jerk performance was also examined, in the presence of external disturbances for the pitching and yawing motions. As mentioned earlier, designers try to reduce the body jerk effect to reduce exposure to undesired motions to achieve effective stability of the dynamic system. Therefore, it is one of the main aims of the study to improve the body jerk performance using one of the proposed IAFC-based control schemes and compare its effectiveness with the conventional PID controller. Among the previously intelligent proposed control strategies, the PID-AFC-IL strategy was explicitly exploited to test the effectiveness of the IAFC scheme on body jerk performance. Here, the pulsating and random noise disturbances were applied as external disturbances. Three cases were studied in relation to the body jerk performance, with reference to equation (12), i.e., PID without any disturbances, PID with disturbances, and PID-AFC-IL with disturbances. The responses of the body jerk performance for these three schemes are presented in **Figures 14** and **15**.

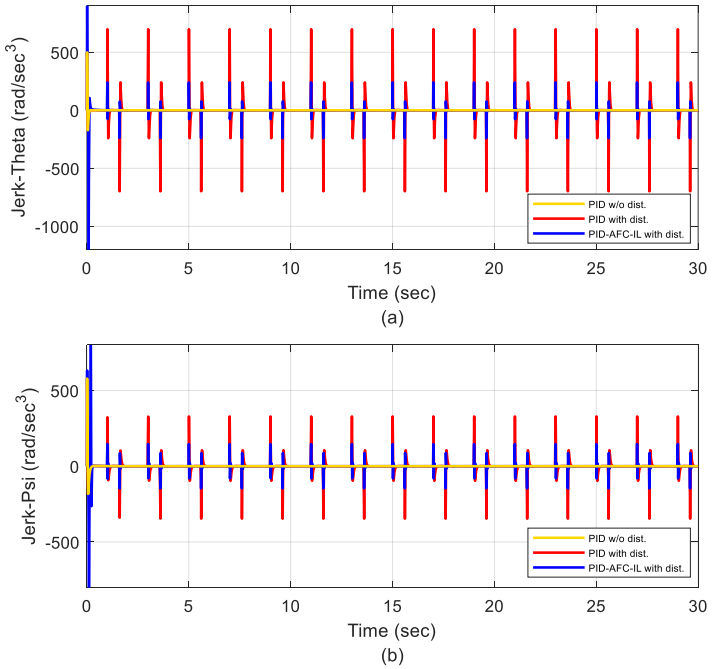

Figure 14. Responses of the body jerk performance in the presence of pulsating disturbance for the motions related to (a) pitch and (b) yaw

Here, the root mean square (RMS) level of output signals was used to deduce the best result where the lower the RMS level, it demonstrates the best performance of the proposed methods. Therefore, the RMS level can be expressed as:

$$\text{RMS} = \sqrt{\frac{1}{N}\sum_{i=1}^{N}[x_i]^2} \tag{29}$$

Where N is the sample size and x the output signal whether pitching and yawing motions.

To obtain an expressive value of the body jerk performance, the percentage of the root mean square (RMS) error value was calculated where the case related to the PID system without disturbances was considered as the reference for comparison for the other two cases to obtain the improvement percentage, as listed in **Tables 7** and **8**.

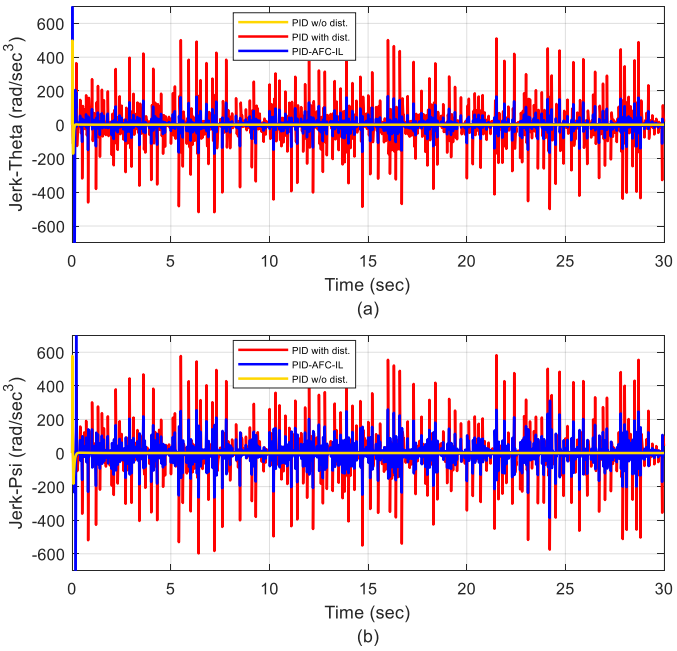

Figure 15. Responses of the body jerk performance in the presence of sinusoidal wave for the motions related to (a) pitch and (b) yaw

Table 7. Characteristics of the 2-D helicopter dynamics with pulsating disturbance

	Motion	RMS value	Improvement Percentage %
PID without Disturbances	θ	11.344	-
	ψ	15.473	-
PID with Disturbances	θ	86.767	87
	ψ	45.237	65.7
PID-ILAFC with Disturbances	θ	39.917	71.5
	ψ	36.652	57.7

Table 8. Characteristics of the 2-D helicopter dynamics with random noise disturbance

	Motion	RMS value	Improvement Percentage %
PID without Disturbances	θ	11.344	-
	ψ	15.473	-
PID with Disturbances	θ	91.29	87.5
	ψ	105.53	85.3
PID-AFC-IL with Disturbances	θ	36.374	68.8
	ψ	48.197	67.8

From **Figures 14** and **15**, the simulated results demonstrate the ability of the IAFC-based controller in improving the body jerk performance by reducing the RMS error value of the pitching and yawing motions. From **Tables 7** and **8**,

in relation to the PID-AFC-IL with disturbances, the percentages of the improvement in the body jerk performance, for pitch (θ) and yaw motions (ψ), are around 54% and 19%, respectively, for the pulsating disturbance, whereas they are 60% and 54%, respectively, for the random noise disturbance. It is quite evident that even the body jerk shows some reduced sustained oscillations when utilizing the PID-AFC-IL though the overall performance is by far much better than the PID only counterpart in the presence of external influences.

V. CONCLUSION

External disturbances and stormy environments are some of the challenges that are typically encountered by the twin-rotor helicopter during trajectory tracking. The 2-DOF helicopter being a highly non-linear and complex dynamical system was modeled and analyzed considering the external disturbances and coupling effects. The proposed PID-AFC-IL, PID-AFC-FL, and ST-PID-AFC schemes, that described the IAFC-based controller, have been successfully designed and implemented to analyze the system behavior and their effectiveness has been benchmarked with the designed PID-AFC and PID control systems. The AFC-based control schemes clearly demonstrate the robust performance in stabilizing the aerial model and rejecting the different types of introduced disturbances, i.e., the sinusoidal wave, pulsating, and random noise disturbances in comparison to the conventional PID controller counterpart. Furthermore, for the body jerk performance related to the pitching and yawing motions, the IAFC-based control structure shows a notable percentage improvement of at least 54% and 19%, respectively, for the pulsating disturbance, and 60% and 54%, respectively, for the random noise disturbance. Future works should focus on the practical implementation of the IAFC-based non-linear control strategies on rotorcraft UAVs for verification and validation of the proposed schemes. This will be very useful to further evaluate the viability of the proposed methods by introducing the non-linear control units, considering various operating and loading conditions.

REFERENCES

Abdelkader, K., Kais, B., 2019. Robust H∞ Gain Neuro-Adaptive Observer Design For Nonlinear Uncertain Systems. Trans. Inst. Meas. Control 41, 2293–2309. https://doi.org/10.1177/0142331218798685

Abdelmaksoud, S.I., Mailah, M., Abdallah, A.M., 2021. Practical Real-Time Implementation of A Disturbance Rejection Control Scheme for A Twin-Rotor Helicopter System Using Intelligent Active Force Control. IEEE Access 9, 4886–4901. https://doi.org/10.1109/ACCESS.2020.3046728

Abdelmaksoud, S. I., Mailah, M., Abdallah, A.M., 2020. Control Strategies and Novel Techniques for Autonomous Rotorcraft Unmanned Aerial Vehicles: A Review. IEEE Access 8, 195142–195169. https://doi.org/10.1109/ACCESS.2020.3031326

Abdelmaksoud, Sherif I., Mailah, M., Abdallah, A.M., 2020. Robust Intelligent Self-Tuning Active Force Control of A Quadrotor With Improved Body Jerk Performance. IEEE Access 8, 150037–150050. https://doi.org/10.1109/ACCESS.2020.3015101

Almtireen, N., Elmoaqet, H., Ryalat, M., 2018. Linearized Modelling and Control for A Twin Rotor System. Autom. Control Comput. Sci. 52, 539–551. https://doi.org/10.3103/S0146411618060020

Arimoto, S., Kawamura, S., Miyazaki, F., 1986. Convergence, Stability and Robustness of Learning Control Schemes for Robot Manipulators, in: Proceedings of the International Symposium on Robot Manipulators on Recent Trends in Robotics: Modeling, Control and Education. Elsevier North-Holland, Inc., New York, NY, USA, pp. 307–316.

Burdess, J.S., Hewit, J.R., 1986. An Active Method for The Control of Mechanical Systems in The Presence of Unmeasurable Forcing. Mech. Mach. Theory 21, 393–400. https://doi.org/10.1016/0094-114X(86)90087-X

Chi, N.V., 2017. Adaptive Feedback Linearization Control for Twin Rotor Multiple-Input Multiple-Output System. Int. J. Control Autom. Syst. 15, 1267–1274. https://doi.org/10.1007/s12555-015-0245-2

Choudhary, S.K., 2016. Optimal Feedback Control of Twin Rotor MIMO System with A Prescribed Degree of Stability. Int. J. Intell. Unmanned Syst. 4, 226–238. https://doi.org/10.1108/IJIUS-07-2016-0005

Eager, D., Pendrill, A.-M., Reistad, N., 2016. Beyond Velocity and Acceleration: Jerk, Snap and Higher Derivatives. Eur. J. Phys. 37, 11 pages. https://doi.org/10.1088/0143-0807/37/6/065008

Faris, F., Moussaoui, A., Djamel, B., Mohammed, T., 2017. Design and Real-Time Implementation of A Decentralized Sliding Mode Controller For Twin Rotor Multi-Input Multi-Output System. Proc. Inst. Mech. Eng. Part J. Syst. Control Eng. 231, 3–13. https://doi.org/10.1177/0959651816680457

Harshath, K., Manoharan, P.S., Varatharajan, M., 2016. Model Predictive Control of TRMS, in: 2016 Biennial International Conference on Power and Energy Systems: Towards Sustainable Energy (PESTSE). Presented

at the 2016 Biennial International Conference on Power and Energy Systems: Towards Sustainable Energy (PESTSE), pp. 1–5. https://doi.org/10.1109/PESTSE.2016.7516455

Hashim, H.A., Abido, M.A., 2015. Fuzzy Controller Design Using Evolutionary Techniques for Twin Rotor MIMO System: A Comparative Study. Comput. Intell. Neurosci. https://doi.org/10.1155/2015/704301

Hewit, J.R., Burdess, J.S., 1981. Fast Dynamic Decoupled Control for Robotics, Using Active Force Control. Mech. Mach. Theory 16, 535–542. https://doi.org/10.1016/0094-114X(81)90025-2

Ijaz, S., Hamayun, M.T., Yan, L., Mumtaz, M.F., 2016. Fractional Order Modeling and Control of Twin Rotor Aero Dynamical System Using Nelder Mead Optimization. J. Electr. Eng. Technol. 11, 1863–1871.

Ilyas, M., Abbas, N., UbaidUllah, M., Imtiaz, W.A., Shah, M. a. Q., Mahmood, K., 2016. Control Law Design for Twin Rotor MIMO System with Nonlinear Control Strategy. Discrete Dyn. Nat. Soc. 2016, 10 pages. https://doi.org/10.1155/2016/2952738

Lin, C.-W., Li, T.-H.S., Chen, C.-C., 2018. Feedback Linearization and Feedforward Neural Network Control with Application to Twin Rotor Mechanism. Trans. Inst. Meas. Control 40, 351–362. https://doi.org/10.1177/0142331216656758

Mailah, M., 1998. Intelligent Active Force Control of A Rigid Robot Arm Using Neural Network and Iterative Learning Algorithms. University of Dundee.

Maiti, R., Sharma, K.D., Sarkar, G., 2018. PSO Based Parameter Estimation and PID Controller Tuning for 2-DOF Nonlinear Twin Rotor MIMO System. Int. J. Autom. Control 12, 582–609. https://doi.org/10.1504/IJAAC.2018.095109

Mascaró Palliser, R., Costa-Castelló, R., Ramos, G.A., 2017. Iterative Learning Control Experimental Results in Twin-Rotor Device. Math. Probl. Eng. 2017, 12 pages. https://doi.org/10.1155/2017/6519497

Meon, M.S., Mohamed, T.L.T., Ramli, M.H.M., Mohamed, M.Z., Manan, N.F.A., 2012. Review and Current Study on New Approach Using PID Active Force Control (PIDAFC) of Twin Rotor Multi Input Multi Output System (TRMS), in: 2012 IEEE Symposium on Humanities, Science and Engineering Research. Presented at the 2012 IEEE Symposium on Humanities, Science and Engineering Research, pp. 163–167. https://doi.org/10.1109/SHUSER.2012.6268848

Omar, M., Mailah, M., Abdelmaksoud, S.I., 2017. Robust Active Force Control of A Quadcopter. J. Mek. 40, 12–22.

Pandey, S.K., Dey, J., Banerjee, S., 2018. Design of Robust Proportional–Integral–Derivative Controller for Generalized Decoupled Twin Rotor Multi-Input-Multi-Output System with Actuator Non-Linearity. Proc. Inst. Mech. Eng. Part J. Syst. Control Eng. 232, 971–982. https://doi.org/10.1177/0959651818771487

Precup, R.-E., Radac, M.-B., Roman, R.-C., Petriu, E.M., 2017. Model-Free Sliding Mode Control of Nonlinear Systems: Algorithms and Experiments. Inf. Sci. 381, 176–192. https://doi.org/10.1016/j.ins.2016.11.026

Raghavan, R., Thomas, S., 2017. Practically Implementable Model Predictive Controller for A Twin Rotor Multi-Input Multi-Output System. J. Control Autom. Electr. Syst. 28, 358–370. https://doi.org/10.1007/s40313-017-0311-5

Rakhtala, S.M., Ahmadi, M., 2017. Twisting Control Algorithm for The Yaw and Pitch Tracking of A Twin Rotor UAV. Int. J. Autom. Control 11, 143–163. https://doi.org/10.1504/IJAAC.2017.083296

Ramli, H., Kuntjoro, W., Meon, M.S., Ishak, K.M.A.K., 2013. Adaptive Active Force Control Application to Twin Rotor Mimo System. Appl. Mech. Mater. 393, 688–693. https://doi.org/10.4028/www.scientific.net/AMM.393.688

Rashad, R., Aboudonia, A., El-Badawy, A., 2016. A Novel Disturbance Observer-Based Backstepping Controller with Command Filtered Compensation for A MIMO System. J. Frankl. Inst. 16, 4039–4061. https://doi.org/10.1016/j.jfranklin.2016.07.017

Rashad, R., El-Badawy, A., Aboudonia, A., 2017. Sliding Mode Disturbance Observer-Based Control of A Twin Rotor MIMO System. ISA Trans. 69, 166–174. https://doi.org/10.1016/j.isatra.2017.04.013

Sabzehmeidani, Y., Mailah, M., Hing, T.H., Abdelmaksoud, S.I., 2021. A Novel Voice-Coil Actuated Mini Crawler for In-Pipe Application Employing Active Force Control with Iterative Learning Algorithm. IEEE Access 9, 28156–28166. https://doi.org/10.1109/ACCESS.2021.3058312

Tahmasebi, M., Mailah, M., Gohari, M., Abd Rahman, R., 2017. Vibration Suppression of Sprayer Boom Structure Using Active Torque Control and Iterative Learning. Part I: Modelling and Control Via Simulation. J. Vib. Control 24, 4689–4699. https://doi.org/10.1177/1077546317733164

Van, C.N., 2016. Designing the Adaptive Tracking Controller for Uncertain Fully Actuated Dynamical Systems with Additive Disturbances Based on Sliding Mode. J. Control Sci. Eng. 2016, 11 pages. https://doi.org/10.1155/2016/9810251

Witczak, M., Buciakowski, M., Puig, V., Rotondo, D., Nejjari, F., 2016. An LMI Approach to Robust Fault Estimation for A Class of Nonlinear Systems. Int. J. Robust Nonlinear Control 26, 1530–1548. https://doi.org/10.1002/rnc.3365

Xin, Y., Qin, Z.-C., Sun, J.-Q., 2019. Input-Output Tracking Control of A 2-DOF Laboratory Helicopter with Improved Algebraic Differential Estimation. Mech. Syst. Signal Process. 116, 843–857. https://doi.org/10.1016/j.ymssp.2018.07.027

Xu, J.-X., Tan, Y., 2003. Linear and Nonlinear Iterative Learning Control, Lecture Notes in Control and Information Sciences. Springer-Verlag, Berlin Heidelberg.

Yang, X., Cui, J., Lao, D., Li, D., Chen, J., 2016. Input Shaping Enhanced Active Disturbance Rejection Control for A Twin Rotor Multi-Input Multi-Output System (TRMS). ISA Trans. 62, 287–298. https://doi.org/10.1016/j.isatra.2016.02.001

Zeghlache, S., Amardjia, N., 2018. Real Time Implementation of Non Linear Observer-Based Fuzzy Sliding Mode Controller for A Twin Rotor Multi-Input Multi-Output System (TRMS). Optik 156, 391–407. https://doi.org/10.1016/j.ijleo.2017.11.053

Zeghlache, S., Kara, K., Saigaa, D., 2014. Type-2 Fuzzy Logic Control of A 2-DOF Helicopter (TRMS System). Cent. Eur. J. Eng. 4, 303–315. https://doi.org/10.2478/s13531-013-0157-y

Zhen-Yu Zhao, Tomizuka, M., Isaka, S., 1993. Fuzzy Gain Scheduling of PID Controllers. IEEE Trans. Syst. Man Cybern. 23, 1392–1398. https://doi.org/10.1109/21.260670